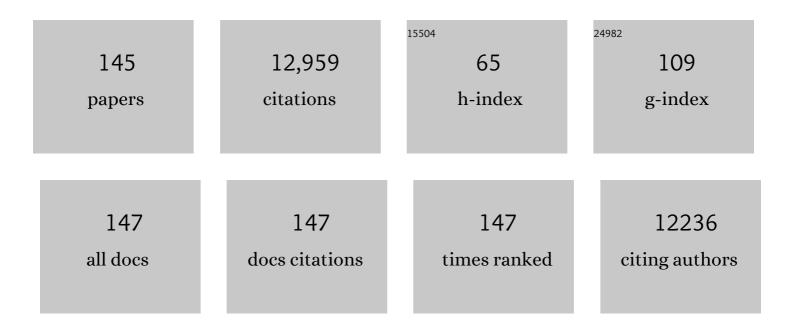
List of Publications by Year in descending order

Source: https://exaly.com/author-pdf/106157/publications.pdf Version: 2024-02-01



#	Article	lF	CITATIONS
1	Self-catalyzed growth of Zn/Co-N-C carbon nanotubes derived from metal-organic frameworks as efficient oxygen reduction catalysts for Zn-air battery. Science China Materials, 2022, 65, 653-662.	6.3	42
2	Self-sacrificial template synthesis of Fe, N co-doped porous carbon as efficient oxygen reduction electrocatalysts towards Zn-air battery application. Chinese Chemical Letters, 2022, 33, 2171-2177.	9.0	26
3	Ni2P nanosheet array for high-efficiency electrohydrogenation of nitrite to ammonia at ambient conditions. Journal of Colloid and Interface Science, 2022, 606, 1055-1063.	9.4	62
4	CoFe-LDH nanowire arrays on graphite felt: A high-performance oxygen evolution electrocatalyst in alkaline media. Chinese Chemical Letters, 2022, 33, 890-892.	9.0	110
5	Loading Singleâ€Ni Atoms on Assembled Hollow Nâ€Rich Carbon Plates for Efficient CO ₂ Electroreduction. Advanced Materials, 2022, 34, e2105204.	21.0	100
6	Fe3S4@reduced graphene oxide composites as novel anode materials for high performance alkaline secondary batteries. Journal of Alloys and Compounds, 2022, 895, 162593.	5.5	3
7	MnO2 nanoarray with oxygen vacancies: An efficient catalyst for NO electroreduction to NH3 at ambient conditions. Materials Today Physics, 2022, 22, 100586.	6.0	54
8	Electrocatalysis enabled transformation of earth-abundant water, nitrogen and carbon dioxide for a sustainable future. Materials Advances, 2022, 3, 1359-1400.	5.4	17
9	Biomass Juncus derived carbon decorated with cobalt nanoparticles enables high-efficiency ammonia electrosynthesis by nitrite reduction. Journal of Materials Chemistry A, 2022, 10, 2842-2848.	10.3	47
10	A gradient hexagonal-prism Fe ₃ Se ₄ @SiO ₂ @C configuration as a highly reversible sodium conversion anode. Journal of Materials Chemistry A, 2022, 10, 4087-4099.	10.3	46
11	Highly efficient two-electron electroreduction of oxygen into hydrogen peroxide over Cu-doped TiO2. Nano Research, 2022, 15, 3880-3885.	10.4	38
12	Ambient Ammonia Synthesis via Electrochemical Reduction of Nitrate Enabled by NiCo ₂ O ₄ Nanowire Array. Small, 2022, 18, e2106961.	10.0	171
13	In situ grown Fe3O4 particle on stainless steel: A highly efficient electrocatalyst for nitrate reduction to ammonia. Nano Research, 2022, 15, 3050-3055.	10.4	108
14	Fabricating N, S Coâ€Doped Hierarchical Macroâ€Mesoâ€Micro Carbon Materials as pHâ€Universal ORR Electrocatalysts**. ChemistrySelect, 2022, 7, .	1.5	8
15	Favorable pore size distribution of biomass-derived N, S dual-doped carbon materials for advanced oxygen reduction reaction. International Journal of Hydrogen Energy, 2022, 47, 12964-12974.	7.1	18
16	High-Performance Electrochemical Nitrate Reduction to Ammonia under Ambient Conditions Using a FeOOH Nanorod Catalyst. ACS Applied Materials & Interfaces, 2022, 14, 17312-17318.	8.0	58
17	Novel 3D Printed Vortex-like Flexible Roller-Compacted Triboelectric Nanogenerator for Self-Powered Electrochemical Degradation of Organic Contaminants. ACS Applied Materials & Interfaces, 2022, 14, 17426-17433.	8.0	13
18	Flower-like open-structured polycrystalline copper with synergistic multi-crystal plane for efficient electrocatalytic reduction of nitrate to ammonia. Nano Energy, 2022, 97, 107124.	16.0	125

#	Article	IF	CITATIONS
19	Cotton-assisted dual rotor-stator triboelectric nanogenerator for real-time monitoring of crop growth environment. Nano Energy, 2022, 101, 107578.	16.0	17
20	Recent Advances in 1D Electrospun Nanocatalysts for Electrochemical Water Splitting. Small Structures, 2021, 2, 2000048.	12.0	157
21	Rational design of carbon materials as anodes for potassium-ion batteries. Energy Storage Materials, 2021, 34, 483-507.	18.0	130
22	Sustainable self-powered electro-Fenton degradation using N, S co-doped porous carbon catalyst fabricated with adsorption-pyrolysis-doping strategy. Nano Energy, 2021, 81, 105623.	16.0	43
23	Pore-structure regulation of biomass-derived carbon materials for an enhanced supercapacitor performance. Nanoscale, 2021, 13, 10051-10060.	5.6	47
24	CoTe nanoparticle-embedded N-doped hollow carbon polyhedron: an efficient catalyst for H ₂ O ₂ electrosynthesis in acidic media. Journal of Materials Chemistry A, 2021, 9, 21703-21707.	10.3	29
25	A treasure map for nonmetallic catalysts: optimal nitrogen and fluorine distribution of biomass-derived carbon materials for high-performance oxygen reduction catalysts. Journal of Materials Chemistry A, 2021, 9, 18251-18259.	10.3	31
26	A-site perovskite oxides: an emerging functional material for electrocatalysis and photocatalysis. Journal of Materials Chemistry A, 2021, 9, 6650-6670.	10.3	146
27	Rational Design and Engineering of Oneâ€Dimensional Hollow Nanostructures for Efficient Electrochemical Energy Storage. Angewandte Chemie - International Edition, 2021, 60, 20102-20118.	13.8	123
28	Template-assisted self-activation of mesoporous carbon with active nitrogen/oxygen configurations for sustainable triboelectric nanogenerator powered electro-Fenton degradation. Nano Energy, 2021, 83, 105825.	16.0	25
29	Rational Design and Engineering of Oneâ€Dimensional Hollow Nanostructures for Efficient Electrochemical Energy Storage. Angewandte Chemie, 2021, 133, 20262-20278.	2.0	13
30	Self-powered electro-Fenton degradation system using oxygen-containing functional groups-rich biomass-derived carbon catalyst driven by 3D printed flexible triboelectric nanogenerator. Nano Energy, 2021, 83, 105720.	16.0	19
31	3D printed triboelectric nanogenerator self-powered electro-Fenton degradation of orange IV and crystal violet system using N-doped biomass carbon catalyst with tunable catalytic activity. Nano Energy, 2021, 83, 105824.	16.0	15
32	Ti ₂ O ₃ Nanoparticles with Ti ³⁺ Sites toward Efficient NH ₃ Electrosynthesis under Ambient Conditions. ACS Applied Materials & Interfaces, 2021, 13, 41715-41722.	8.0	89
33	Highâ€Performance Electrochemical NO Reduction into NH ₃ by MoS ₂ Nanosheet. Angewandte Chemie, 2021, 133, 25467-25472.	2.0	102
34	Phosphorized CoNi ₂ S ₄ Yolkâ€Shell Spheres for Highly Efficient Hydrogen Production via Water and Urea Electrolysis. Angewandte Chemie, 2021, 133, 23067-23073.	2.0	14
35	Template-assisted polymerization-pyrolysis derived mesoporous carbon anchored with Fe/Fe3C and Feâ^'NX species as efficient oxygen reduction catalysts for Zn-air battery. International Journal of Hydrogen Energy, 2021, 46, 37895-37906.	7.1	23
36	N, P-dual doped carbonaceous catalysts derived from bifunctional-salt activation for effective electro-Fenton degradation on waterborne organic pollutions. Electrochimica Acta, 2021, 389, 138732.	5.2	8

#	Article	IF	CITATIONS
37	Greatly Facilitated Two-Electron Electroreduction of Oxygen into Hydrogen Peroxide over TiO ₂ by Mn Doping. ACS Applied Materials & Interfaces, 2021, 13, 46659-46664.	8.0	46
38	Highâ€Performance Electrochemical NO Reduction into NH ₃ by MoS ₂ Nanosheet. Angewandte Chemie - International Edition, 2021, 60, 25263-25268.	13.8	180
39	Phosphorized CoNi ₂ S ₄ Yolkâ€Shell Spheres for Highly Efficient Hydrogen Production via Water and Urea Electrolysis. Angewandte Chemie - International Edition, 2021, 60, 22885-22891.	13.8	191
40	Nitrogen, phosphorus, sulfur tri-doped porous carbon derived from covalent polymer with versatile performances in supercapacitor, oxygen reduction reaction and electro-fenton degradation. Microporous and Mesoporous Materials, 2021, 325, 111335.	4.4	18
41	Hierarchical porous biomass-derived carbon framework with ultrahigh surface area for outstanding capacitance supercapacitor. Renewable Energy, 2021, 179, 1826-1835.	8.9	48
42	Recent Progress in Electrocatalytic Methanation of CO ₂ at Ambient Conditions. Advanced Functional Materials, 2021, 31, 2009449.	14.9	92
43	Electrocatalytic H ₂ O ₂ production <i>via</i> two-electron O ₂ reduction by Mo-doped TiO ₂ nanocrystallines. Catalysis Science and Technology, 2021, 11, 6970-6974.	4.1	4
44	A MnS/FeS ₂ heterostructure with a high degree of lattice matching anchored into carbon skeleton for ultra-stable sodium-ion storage. Journal of Materials Chemistry A, 2021, 9, 24024-24035.	10.3	38
45	High-efficiency electrohydrogenation of nitric oxide to ammonia on a Ni ₂ P nanoarray under ambient conditions. Journal of Materials Chemistry A, 2021, 9, 24268-24275.	10.3	68
46	Functional integration of hierarchical core–shell architectures <i>via</i> vertically arrayed ultrathin CuSe nanosheets decorated on hollow CuS microcages targeting highly effective sodium-ion storage. Journal of Materials Chemistry A, 2021, 9, 27615-27628.	10.3	56
47	Electrochemical two-electron O ₂ reduction reaction toward H ₂ O ₂ production: using cobalt porphyrin decorated carbon nanotubes as a nanohybrid catalyst. Journal of Materials Chemistry A, 2021, 9, 26019-26027.	10.3	55
48	An ultrasmall Ru ₂ P nanoparticles–reduced graphene oxide hybrid: an efficient electrocatalyst for NH ₃ synthesis under ambient conditions. Journal of Materials Chemistry A, 2020, 8, 77-81.	10.3	115
49	Aqueous electrocatalytic N ₂ reduction for ambient NH ₃ synthesis: recent advances in catalyst development and performance improvement. Journal of Materials Chemistry A, 2020, 8, 1545-1556.	10.3	226
50	FeOOH quantum dots decorated graphene sheet: An efficient electrocatalyst for ambient N2 reduction. Nano Research, 2020, 13, 209-214.	10.4	48
51	Synthesis of Copper‣ubstituted CoS ₂ @Cu _{<i>x</i>} S Double‣helled Nanoboxes by Sequential Ion Exchange for Efficient Sodium Storage. Angewandte Chemie, 2020, 132, 2666-2670.	2.0	29
52	Synthesis of Copperâ€&ubstituted CoS ₂ @Cu _{<i>x</i>} S Doubleâ€&helled Nanoboxes by Sequential Ion Exchange for Efficient Sodium Storage. Angewandte Chemie - International Edition, 2020, 59, 2644-2648.	13.8	182
53	Nitrogenâ€Doped Cobalt Pyrite Yolk–Shell Hollow Spheres for Longâ€Life Rechargeable Zn–Air Batteries. Advanced Science, 2020, 7, 2001178.	11.2	206
54	Metal-based electrocatalytic conversion of CO ₂ to formic acid/formate. Journal of Materials Chemistry A, 2020, 8, 21947-21960.	10.3	125

#	Article	IF	CITATIONS
55	Electrocatalytic N2 reduction to NH3 with high Faradaic efficiency enabled by vanadium phosphide nanoparticle on V foil. Nano Research, 2020, 13, 2967-2972.	10.4	45
56	Enabling electrochemical conversion of N ₂ to NH ₃ under ambient conditions by a CoP ₃ nanoneedle array. Journal of Materials Chemistry A, 2020, 8, 17956-17959.	10.3	53
57	Threeâ€Dimensional SnS ₂ Nanoarrays with Enhanced Lithiumâ€lon Storage Properties. ChemElectroChem, 2020, 7, 4484-4491.	3.4	8
58	Iron-based phosphides as electrocatalysts for the hydrogen evolution reaction: recent advances and future prospects. Journal of Materials Chemistry A, 2020, 8, 19729-19745.	10.3	295
59	Oxidationâ€etching induced morphology regulation of Cu catalysts for highâ€performance electrochemical <scp>N₂</scp> reduction. EcoMat, 2020, 2, e12026.	11.9	13
60	Engineering flexible 3D printed triboelectric nanogenerator to self-power electro-Fenton degradation of pollutants. Nano Energy, 2020, 74, 104908.	16.0	54
61	High-performance non-enzymatic glucose detection: using a conductive Ni-MOF as an electrocatalyst. Journal of Materials Chemistry B, 2020, 8, 5411-5415.	5.8	170
62	Recent advances in electrospun one-dimensional carbon nanofiber structures/heterostructures as anode materials for sodium ion batteries. Journal of Materials Chemistry A, 2020, 8, 11493-11510.	10.3	113
63	A cobalt–phosphorus nanoparticle decorated N-doped carbon nanosheet array for efficient and durable hydrogen evolution at alkaline pH. Sustainable Energy and Fuels, 2020, 4, 3884-3887.	4.9	127
64	Identifying the Origin of Ti ³⁺ Activity toward Enhanced Electrocatalytic N ₂ Reduction over TiO ₂ Nanoparticles Modulated by Mixedâ€Valent Copper. Advanced Materials, 2020, 32, e2000299.	21.0	278
65	Effects of gold nanoparticle morphologies on interactions with proteins. Materials Science and Engineering C, 2020, 111, 110830.	7.3	35
66	Designed Formation of Double‧helled Ni–Fe Layeredâ€Doubleâ€Hydroxide Nanocages for Efficient Oxygen Evolution Reaction. Advanced Materials, 2020, 32, e1906432.	21.0	305
67	Sn dendrites for electrocatalytic N ₂ reduction to NH ₃ under ambient conditions. Sustainable Energy and Fuels, 2020, 4, 4469-4472.	4.9	54
68	Greatly Enhanced Electrocatalytic N ₂ Reduction over V ₂ O ₃ /C by P Doping. ChemNanoMat, 2020, 6, 1315-1319.	2.8	71
69	Recent advances in electrospun nanofibers for supercapacitors. Journal of Materials Chemistry A, 2020, 8, 16747-16789.	10.3	166
70	Rationally Designed Three‣ayered Cu ₂ S@Carbon@MoS ₂ Hierarchical Nanoboxes for Efficient Sodium Storage. Angewandte Chemie, 2020, 132, 7245-7250.	2.0	42
71	Rationally Designed Three‣ayered Cu ₂ S@Carbon@MoS ₂ Hierarchical Nanoboxes for Efficient Sodium Storage. Angewandte Chemie - International Edition, 2020, 59, 7178-7183.	13.8	232
72	Platelet-like CuS impregnated with twin crystal structures for high performance sodium-ion storage. Journal of Materials Chemistry A, 2020, 8, 8049-8057.	10.3	38

#	Article	IF	CITATIONS
73	Interfacing Manganese Oxide and Cobalt in Porous Graphitic Carbon Polyhedrons Boosts Oxygen Electrocatalysis for Zn–Air Batteries. Advanced Materials, 2019, 31, e1902339.	21.0	363
74	Pyrrolic-nitrogen-rich biomass-derived catalyst for sustainable degradation of organic pollutant via a self-powered electro-Fenton process. Nano Energy, 2019, 64, 103940.	16.0	62
75	Why and how to tailor the vertical coordinate of pore size distribution to construct ORR-active carbon materials?. Nano Energy, 2019, 58, 384-391.	16.0	97
76	A general dual-templating approach to biomass-derived hierarchically porous heteroatom-doped carbon materials for enhanced electrocatalytic oxygen reduction. Energy and Environmental Science, 2019, 12, 648-655.	30.8	318
77	Ambient electrohydrogenation of N ₂ for NH ₃ synthesis on non-metal boron phosphide nanoparticles: the critical role of P in boosting the catalytic activity. Journal of Materials Chemistry A, 2019, 7, 16117-16121.	10.3	105
78	A universal strategy for carbon–based ORR–active electrocatalyst: One porogen, two pore–creating mechanisms, three pore types. Nano Energy, 2019, 62, 628-637.	16.0	91
79	Self-power electroreduction of N2 into NH3 by 3D printed triboelectric nanogenerators. Materials Today, 2019, 28, 17-24.	14.2	127
80	Surface chemistry of gold nanoparticles determines interactions with bovine serum albumin. Materials Science and Engineering C, 2019, 103, 109856.	7.3	39
81	Sustainable self-powered electro-Fenton degradation of organic pollutants in wastewater using carbon catalyst with controllable pore activated by EDTA-2Na. Nano Energy, 2019, 59, 346-353.	16.0	51
82	PdP ₂ nanoparticles–reduced graphene oxide for electrocatalytic N ₂ conversion to NH ₃ under ambient conditions. Journal of Materials Chemistry A, 2019, 7, 24760-24764.	10.3	81
83	Synthesis of Cobalt Sulfide Multiâ€shelled Nanoboxes with Precisely Controlled Two to Five Shells for Sodiumâ€ion Batteries. Angewandte Chemie, 2019, 131, 2701-2705.	2.0	29
84	Synthesis of Cobalt Sulfide Multiâ€shelled Nanoboxes with Precisely Controlled Two to Five Shells for Sodiumâ€ion Batteries. Angewandte Chemie - International Edition, 2019, 58, 2675-2679.	13.8	182
85	Preparation of porous carbon electrodes from semen cassiae for high-performance electric double-layer capacitors. New Journal of Chemistry, 2018, 42, 6763-6769.	2.8	29
86	An advanced electro-Fenton degradation system with triboelectric nanogenerator as electric supply and biomass-derived carbon materials as cathode catalyst. Nano Energy, 2018, 45, 21-27.	16.0	77
87	Marriage of an Ether-Based Electrolyte with Hard Carbon Anodes Creates Superior Sodium-Ion Batteries with High Mass Loading. ACS Applied Materials & Interfaces, 2018, 10, 41380-41388.	8.0	76
88	Nickel–Iron Layered Double Hydroxide Hollow Polyhedrons as a Superior Sulfur Host for Lithium–Sulfur Batteries. Angewandte Chemie - International Edition, 2018, 57, 10944-10948.	13.8	269
89	Nickel–Iron Layered Double Hydroxide Hollow Polyhedrons as a Superior Sulfur Host for Lithium–Sulfur Batteries. Angewandte Chemie, 2018, 130, 11110-11114.	2.0	35
90	Ambient N2 fixation to NH3 at ambient conditions: Using Nb2O5 nanofiber as a high-performance electrocatalyst. Nano Energy, 2018, 52, 264-270.	16.0	331

#	Article	IF	CITATIONS
91	Hierarchically porous carbon materials with controllable proportion of micropore area by dual-activator synthesis for high-performance supercapacitors. Journal of Materials Chemistry A, 2018, 6, 15340-15347.	10.3	116
92	Self-Powered Electrochemical Oxidation of 4-Aminoazobenzene Driven by a Triboelectric Nanogenerator. ACS Nano, 2017, 11, 770-778.	14.6	53
93	A versatile biomass derived carbon material for oxygen reduction reaction, supercapacitors and oil/water separation. Nano Energy, 2017, 33, 334-342.	16.0	352
94	Triboelectric Nanogenerator Powered Electrochemical Degradation of Organic Pollutant Using Pt-Free Carbon Materials. ACS Nano, 2017, 11, 3965-3972.	14.6	91
95	N-doped-carbon-coated Fe3O4 from metal-organic framework as efficient electrocatalyst for ORR. Nano Energy, 2017, 40, 462-470.	16.0	198
96	Chemical crosslinking engineered nitrogen-doped carbon aerogels from polyaniline-boric acid-polyvinyl alcohol gels for high-performance electrochemical capacitors. Carbon, 2017, 123, 471-480.	10.3	43
97	An innovative electro-fenton degradation system self-powered by triboelectric nanogenerator using biomass-derived carbon materials as cathode catalyst. Nano Energy, 2017, 42, 314-321.	16.0	71
98	Biomass-derived interconnected carbon nanoring electrochemical capacitors with high performance in both strongly acidic and alkaline electrolytes. Journal of Materials Chemistry A, 2017, 5, 181-188.	10.3	130
99	Selfâ€Powered Electrochemistry for the Oxidation of Organic Molecules by a Cross‣inked Triboelectric Nanogenerator. Advanced Materials, 2016, 28, 5188-5194.	21.0	31
100	Self-assembly-template engineering nitrogen-doped carbon aerogels for high-rate supercapacitors. Nano Energy, 2016, 28, 206-215.	16.0	174
101	Electrochemical oxidation degradation of azobenzene dye self-powered by multilayer-linkage triboelectric nanogenerator. Nano Energy, 2016, 30, 52-58.	16.0	27
102	Nitrogen-Doped Porous Carbon Derived from Malachium Aquaticum Biomass as a Highly Efficient Electrocatalyst for Oxygen Reduction Reaction. Electrochimica Acta, 2016, 220, 427-435.	5.2	73
103	Functional Groups and Pore Size Distribution Do Matter to Hierarchically Porous Carbons as High-Rate-Performance Supercapacitors. Chemistry of Materials, 2016, 28, 445-458.	6.7	221
104	Honeysuckles-derived porous nitrogen, sulfur, dual-doped carbon as high-performance metal-free oxygen electroreduction catalyst. Nano Energy, 2015, 12, 785-793.	16.0	167
105	Nitrogen-doped carbon shell structure derived from natural leaves as a potential catalyst for oxygen reduction reaction. Nano Energy, 2015, 13, 518-526.	16.0	132
106	Recycling the biowaste to produce nitrogen and sulfur self-doped porous carbon as an efficient catalyst for oxygen reduction reaction. Nano Energy, 2015, 16, 408-418.	16.0	119
107	Peanut-Shell-like Porous Carbon from Nitrogen-Containing Poly- <i>N</i> -phenylethanolamine for High-Performance Supercapacitor. ACS Applied Materials & Interfaces, 2015, 7, 22238-22245.	8.0	61
108	Self-assembly of cuprous oxide nanoparticles supported on reduced graphene oxide and their enhanced performance for catalytic reduction of nitrophenols. RSC Advances, 2015, 5, 71259-71267.	3.6	36

#	Article	IF	CITATIONS
109	Oxidation of diclofenac by potassium ferrate (VI): Reaction kinetics and toxicity evaluation. Science of the Total Environment, 2015, 506-507, 252-258.	8.0	35
110	Transforming organic-rich amaranthus waste into nitrogen-doped carbon with superior performance of the oxygen reduction reaction. Energy and Environmental Science, 2015, 8, 221-229.	30.8	307
111	Large scale production of biomass-derived N-doped porous carbon spheres for oxygen reduction and supercapacitors. Journal of Materials Chemistry A, 2014, 2, 3317.	10.3	208
112	Nitrogen-enriched carbon from bamboo fungus with superior oxygen reduction reaction activity. Journal of Materials Chemistry A, 2014, 2, 18263-18270.	10.3	78
113	A green one-arrow-two-hawks strategy for nitrogen-doped carbon dots as fluorescent ink and oxygen reduction electrocatalysts. Journal of Materials Chemistry A, 2014, 2, 6320.	10.3	136
114	Nitrogenâ€Doped Carbon with Mesopore Confinement Efficiently Enhances the Tolerance, Sensitivity, and Stability of a Pt Catalyst for the Oxygen Reduction Reaction. Particle and Particle Systems Characterization, 2013, 30, 864-872.	2.3	27
115	CoS2–graphene composite as efficient catalytic counter electrode for dye-sensitized solar cell. Electrochimica Acta, 2013, 114, 173-179.	5.2	71
116	Old tree with new shoots: silver nanoparticles for label-free and colorimetric mercury ions detection. Journal of Nanoparticle Research, 2013, 15, 1.	1.9	28
117	Effects of precursor treatment on the structure and electrochemical properties of spinel LiMn2O4 cathode. Journal of Alloys and Compounds, 2013, 566, 16-21.	5.5	20
118	Application of hierarchical TiO2 spheres as scattering layer for enhanced photovoltaic performance in dye sensitized solar cell. CrystEngComm, 2013, 15, 3351.	2.6	52
119	One stone, two birds: Gastrodia elata-derived heteroatom-doped carbon materials for efficient oxygen reduction electrocatalyst and as fluorescent decorative materials. Nano Energy, 2013, 2, 1261-1270.	16.0	54
120	Anatase TiO ₂ nanocrystals enclosed by well-defined crystal facets and their application in dye-sensitized solar cell. CrystEngComm, 2013, 15, 516-523.	2.6	35
121	Hierarchically micro/nanostructured porous metallic copper: Convenient growth and superhydrophilic and catalytic performance. Journal of Materials Chemistry, 2012, 22, 21733.	6.7	64
122	Bioinspired synthesis of hierarchically micro/nano-structured Cul tetrahedron and its potential application as adsorbent for Cd(II) with high removal capacity. Journal of Hazardous Materials, 2012, 211-212, 55-61.	12.4	14
123	Hierarchical plasmonic-metal/semiconductor micro/nanostructures: green synthesis and application in catalytic reduction of p-nitrophenol. Journal of Nanoparticle Research, 2012, 14, 1.	1.9	31
124	Antibiotic-inspired zinc oxide with morphology-dependent photocatalytic activity. Canadian Journal of Chemistry, 2011, 89, 590-597.	1.1	3
125	Biomolecule-assisted in situ route toward 3D superhydrophilic Ag/CuO micro/nanostructures with excellent artificial sunlight self-cleaning performance. Journal of Materials Chemistry, 2011, 21, 7281.	6.7	39
126	Recent developments and applications of hybrid surface plasmon resonance interfaces in optical sensing. Analytical and Bioanalytical Chemistry, 2011, 399, 91-101.	3.7	12

#	Article	IF	CITATIONS
127	Hierarchical Ag/ZnO micro/nanostructure: Green synthesis and enhanced photocatalytic performance. Journal of Solid State Chemistry, 2011, 184, 764-769.	2.9	94
128	Cauliflower-like CuI nanostructures: Green synthesis and applications as catalyst and adsorbent. Materials Science and Engineering B: Solid-State Materials for Advanced Technology, 2011, 176, 1021-1027.	3.5	24
129	Highly Stable Au Nanoparticles with Tunable Spacing and Their Potential Application in Surface Plasmon Resonance Biosensors. Advanced Functional Materials, 2010, 20, 78-86.	14.9	67
130	Bioinspired Green Synthesis of Nanomaterials and their Applications. Current Nanoscience, 2010, 6, 452-468.	1.2	12
131	Bioinspired synthesis of well faceted CuI nanostructures and evaluation of their catalytic performance for coupling reactions. Green Chemistry, 2010, 12, 1442.	9.0	24
132	Preparation and characterization of PS/pAPBA core-shell microspheres. Frontiers of Chemistry in China: Selected Publications From Chinese Universities, 2009, 4, 168-172.	0.4	2
133	Innovative Platform for Transmission Localized Surface Plasmon Transducers and Its Application in Detecting Heavy Metal Pd(II). Analytical Chemistry, 2009, 81, 7703-7712.	6.5	23
134	Transferrable Superhydrophobic Surface Constructed by a Hexagonal Cul Powder without Modification by Low-Free-Energy Materials. ACS Applied Materials & Interfaces, 2009, 1, 2080-2085.	8.0	19
135	Ordered Co3O4 hierarchical nanorod arrays: tunable superhydrophilicity without UV irradiation and transition to superhydrophobicity. Journal of Materials Chemistry, 2009, 19, 8366.	6.7	129
136	Tyrosine-assisted preparation of Ag/ZnO nanocomposites with enhanced photocatalytic performance and synergistic antibacterial activities. Nanotechnology, 2008, 19, 445711.	2.6	168
137	One-Pot Synthesis of Ag/ZnO Self-Assembled 3D Hollow Microspheres with Enhanced Photocatalytic Performance. Journal of Physical Chemistry C, 2008, 112, 16792-16800.	3.1	331
138	Green Fabrication of Hierarchical CuO Hollow Micro/Nanostructures and Enhanced Performance as Electrode Materials for Lithium-ion Batteries. Journal of Physical Chemistry C, 2008, 112, 19324-19328.	3.1	181
139	Biopolymer-Assisted Synthesis of Single Crystalline Gold Disks by a Hydrothermal Route. Current Nanoscience, 2008, 4, 145-150.	1.2	7
140	ZnO-Based Hollow Microspheres:Â Biopolymer-Assisted Assemblies from ZnO Nanorods. Journal of Physical Chemistry B, 2006, 110, 15847-15852.	2.6	137
141	Engineering white light-emitting Eu-doped ZnO urchins by biopolymer-assisted hydrothermal method. Applied Physics Letters, 2006, 89, 123125.	3.3	108
142	Carboxyl-cored dendrimer and toluene-assisted fabrication of uniform platinum nanodendrites at a water/oil interface and their potential application as a catalyst. Nanotechnology, 2006, 17, 1599-1606.	2.6	5
143	Room-temperature strategy for networked nonspherical gold nanostructures from Au(III)[G-2]CO2H dendrimer complex. Journal of Colloid and Interface Science, 2006, 293, 409-413.	9.4	11
144	Unique gold sponges: biopolymer-assisted hydrothermal synthesis and potential application as surface-enhanced Raman scattering substrates. Nanotechnology, 2005, 16, 2530-2535.	2.6	29

#	Article	IF	CITATIONS
145	Studies on the second virial coefficient of sodium alginate solution. Polymers for Advanced Technologies, 1997, 8, 722-726.	3.2	3